liquids

MDPI

Article

Abraham Model Descriptors for Vitamin K4: Prediction of Solution, Biological and Thermodynamic Properties

Saikiran Motati, Ramya Motati, Trisha Kandi and William E. Acree, Jr. *

Department of Chemistry, University of North Texas, Denton, TX 76203, USA
* Correspondence: bill.acree@unt.edu

Abstract: Spectrophotometric measurements were used to determine the mole fraction solubilities of vitamin K4 dissolved in cyclohexane, methylcyclohexane, 1-heptanol, 2-butanol, 2-pentanol, 2-methyl-1-butanol, 4-methyl-2-pentanol, and cyclopentanol at 298.15 K. Results from our experimental measurements, combined with the published solubility data, are used to calculate the solute descriptors of the vitamin K4 solute. The calculated solute descriptors describe the observed solubility data to within an overall standard deviation of 0.110 log units. The calculated solute descriptors were also used to estimate the several blood-to-rat tissue partition coefficients of vitamin K4, as well as the equilibrium vapor pressure above the solid vitamin at 298 K, and the vitamin's enthalpy of solvation in both water and in 1,4-dioxane organic mono-solvent.

Keywords: vitamin K4; mole fraction solubilities; Abraham model solute descriptors; blood-to-tissue partition coefficients

check for updates

Citation: Motati, S.; Motati, R.; Kandi, T.; Acree, W.E., Jr. Abraham Model Descriptors for Vitamin K4: Prediction of Solution, Biological and Thermodynamic Properties. *Liquids* **2023**, *3*, 402–413. https://doi.org/10.3390/liquids3040025

Academic Editor: Daniel Ricardo Delgado

Received: 11 August 2023
Revised: 12 September 2023
Accepted: 27 September 2023
Published: 2 October 2023

1. Introduction

The pharmaceutical industry faces many challenges in its efforts to bring potential drug candidates successfully through the drug discovery process. Only a small percentage of drug candidates make their way to the market for human consumption. Candidates often fail in the later stages of the discovery process because of poor aqueous solubility and slow dissolution kinetics, which lead to low drug concentration in the gastrointestinal tract and in blood circulation. Low bioavailability adversely affects drug efficacy because higher dosages are needed to provide a sufficient quantity of drug at the target site in order to achieve the desired therapeutic effect. Numerous methods have been suggested to overcome low aqueous solubility, including pH manipulation, addition of organic solvents and complexing agents, nanosuspension modes of delivery, co-crystal formation, and hydrotrope addition. Determining which approach is best for a specific drug molecule is both time-consuming and expensive in terms of employee labor and chemical resources. Several computation methods are available for estimating the solubility of drug candidates [1–9] and to assist researchers in selecting an appropriate organic solvent and mixture composition if co-solvency is needed to enhance a low aqueous solubility [4,6,7,9–13].

Our recent efforts pertaining to solubility have focused on experimental measurements for crystalline nonelectrolyte solutes dissolved in select organic mono-solvents [14–17] and in binary aqueous-organic solvent mixtures [18–22]. The measured solubility data has been used in the calculation of the Abraham model solute descriptors [14–17] and in developing the Abraham model correlations for predicting the solubilities of pharmaceutical compounds in organic solvents used in recrystallization purifications and in co-solvency solubility enhancements [23–27]. Transcutol was one the recent organic solvents for which the predictive Abraham model expressions were reported [23]. We note that the Abraham model enables estimation of many other important pharmaceutical properties besides solubility. Expressions have been reported for human skin permeations from aqueous solutions [28,29], human and animal air-to-blood partition coefficients [30], air-to-lung and

blood-to-lung partition coefficients [31], air-to-muscle and blood-to-muscle distribution coefficients [32], Draize rabbit eye test compatibility and eye irritation thresholds in humans [33], human intestinal absorption of neutral molecules and ionic species [34,35]; air-to-fat and blood-to-fat distribution coefficients of drugs and volatile organic compounds [36], in vivo blood-to-rat brain distribution coefficients [37], in vitro air-to-rat/human brain partition coefficients of volatile organic compounds [38], solute permeabilities from select parallel artificial membrane permeability assay (PAMPA) models [39,40], and water-to-muscle protein partition coefficients [41,42]. The Abraham model correlations have also been used to assist researchers identify organic solvents that can mimic blood [43] and fatty tissue [44] for extraction and leaching studies to test the safety of medical devices that come into direct contact with a patient's body fluids and tissues.

Prediction of each of the fore-mentioned properties using published Abraham model expressions requires a priori knowledge of the descriptor values of the desired solute molecule. Experimental-based solute descriptors are currently available for over 8000 different organic compounds [45]. Easy-to-use software programs [45–47] provide a convenient means to estimate descriptor values for those compounds whose experimental-based values have not been determined. The software programs estimate the Abraham solute descriptors from the molecule's canonical SMILES code. Our experience in using the internet software programs is that the programs provide reasonably good estimations of the Abraham solute descriptors for molecules containing only a few functional groups. Estimated values do differ rather significantly from experimental-based descriptor values as the number of functional groups increase. The programs often fail to properly account for intramolecular hydrogen-bond in that the **A** and **B** solute descriptors are often overestimated. The predictive methods can be no better than the data sets used to train the models. Our comments are not intended to criticize the software programs, but rather to suggest that the best way to improve the predictive capabilities is to increase the chemical diversity of the molecules within the training data sets. We have recently reported experiment-based solute descriptors for four molecules that exhibit intramolecular hydrogen-bond formation [48–50], and for one molecule that contains the *N*-hydroxyl (>N-OH) functional group [15].

In the current communication we continue our efforts to provide the scientific community with experiment-based solute descriptors for additional organic compounds. The compound that we selected to study is vitamin K4 (2-methyl-1,4-napthodiol diacetate; $C_{15}H_{14}O_4$; Chemical Abstracts Registry Number 573-20-6) which a synthetic hydrophylic menadione compound that is clinically used in the treatment of blood clotting disorders. The chemical compound is also reported to exhibit anticancer activity in human prostate carcinoma PC-3 cells [51], and to both inhibit proliferation and induce apoptosis of U20S osteosarcoma cells [52]. The recently published mole fraction solubility data of Lu and coworkers [53] for vitamin K4 in methanol, ethanol, 1-propanol, 2-propanol, 1-butanol, 2-methyl-1-propanol, 1-pentanol, 3-methyl-1-butanol, methyl acetate, ethyl acetate, propyl acetate, butyl acetate, and pentyl acetate provides 13 experimental values for use in the solute descriptor calculations. The published solubility data in cyclohexanol was excluded from the calculations because there is no Abraham model correlation for this organic mono-solvent. We augmented the published data by performing additional solubility measurements in cyclohexane, methylcyclohexane, 1-heptanol, 2-butanol, 2-pentanol, 2-methyl-1-butanol, 4-methyl-2-pentanol, and cyclopentanol at 298.15 K. Cyclohexane and methylcyclohexane were specifically selected because of their non-polar nature and inability to engage in hydrogen-bond formation. Lu and coworkers did not perform solubility measurements in any saturated hydrocarbon solvents. The alcohol solvents were selected for their hydrogen-bonding ability and for the various placements of the -OH and methyl-functional groups within the molecule.

2. Materials and Methods

Vitamin K4 was purchased from a commercial source (TCI America, Portland, OR, USA, 0.98 mass fraction) and recrystallized two times from anhydrous methanol prior to use. The purity of the recrystallized sample of vitamin K4 was 0.997 mass fraction as determined by gas-chromatographic analyses (with thermal conductivity detection). The eight organic solvents were purchased from commercial sources as follows: cyclohexane (Sigma-Aldrich Chemical Company, St. Louis, MO, USA, 0.995 mass fraction, anhydrous), methylcyclohexane (Aldrich Chemical Company, Milwaukee, WI, USA, 0.99+ mass fraction, anhydrous), 2-butanol (Aldrich Chemical Company, 0.995 mass fraction, anhydrous), 2-pentanol (Thermo Scientific, Ward Hill, MA, USA, 0.99 mass fraction), 2-methyl-1-butanol (Sigma-Aldrich Chemical Company, 0.99 mass fraction), 4-methyl-2-pentanol (Acros Organics, Morris Plains, NJ, USA, 0.99+ mass fraction), 1-heptanol (Alfa Aesar, Heysham, UK, 0.99 mass fraction), and cyclopentanol (Sigma-Aldrich Chemical Company, 0.995 mass fraction, anhydrous). All eight solvents were stored over activated molecular sieves shortly before use to remove trace moisture. Gas chromatographic analysis (with thermal conductivity detection) indicated the organic solvent purities to be at least 0.997 mass fraction.

The solubility of vitamin K4 in the eight organic solvents were measured utilizing a static method of equilibration. Mass fraction concentrations in the saturated solutions were calculated from spectroscopic absorbance measurements. The experimental methodology employed in the current communication has been described in earlier publications [54,55] and to conserve journal space we provide only an abbreviated version. Aliquots of the clear saturated solutions were transferred using a heated glass syringe into weighed volumetric flasks after the samples had equilibrated in a constant temperature water bath at 298.15 $\pm$ 0.05 K for at least three days with periodic agitation. The transferred aliquot was weighed on a Mettler Toledo ME104E electronic analytical balance (Mettler Toledo, Columbus, OH, USA) and then diluted quantitatively with 2-propanol. Absorbances of the diluted solutions were recorded at an analysis wavelength of 301 nm on a Milton Roy Spectronic 1000 Plus single-beam spectrophotometer (Milton Roy Company, Rochester, NY, USA). The concentration of each diluted solution was computed from a Beer-Lambert law absorbance versus concentration calibration curve generated from the measured absorbances of nine carefully prepared standard solutions of known vitamin K4 concentration. The calculated molar absorptivity, $\varepsilon \approx 6450/(\text{mol}^{-1}\ \text{cm})$, was constant over the concentration range of 7.83×10^{-5} Molar to 2.61×10^{-4} Molar used in the molar absorptivity determination. Molar concentrations determined from the absorbance measurements were first converted to mass fraction solubilities and then to mole fraction solubilities using the mass of the sample analyzed, molar masses of vitamin K4 and the respective organic mono-solvents, volume of the volumetric flasks, and any dilutions needed to get the measured absorbances to fall on the calibration curve. No evidence of solvent formation or solid phase transformation was observed. Melting point temperatures of the solid samples recovered from the saturated solutions within experimental uncertainty of the melting point temperature of the purified, recrystallized sample.

3. Results and Discussion

The experimental mole fraction solubilities, $x_{\text{S,organic}}$, of vitamin K4 dissolved in eight different organic mono-solvents are reported in Table 1. The tabulated numerical values represent the average of between four and eight independent determinations and were reproducible to within +2.5%. We were not able to find published solubility data in the chemical literature to compare our measured $x_{S,organic}$ against. In fact, the only published solubility data that we found in our search of the published literature was the mole fraction solubilities of vitamin K4 contained in the paper by Lu and coworkers [53]. Experimental values reported in the current study significantly increased the available solubility data for vitamin K4.

Table 1. Experimental mole fraction solubilities of vitamin K4, $x_{S,organic}$, in select organic mono-solvents at 298.15 K.

Organic Mono-Solvent	$x_{S,organic}$
Cyclohexane	0.001713
Methylcyclohexane	0.002215
1-Heptanol	0.006035
2-Butanol	0.005822
2-Pentanol	0.006857
2-Methyl-1-butanol	0.004897
4-Methyl-2-pentanol	0.005729
Cyclopentanol	0.008789

The calculation of the Abraham model solute descriptors is relatively straightforward, provided that one has a sufficient experimental partition coefficient and molar solubility data to construct the needed mathematical equations. To aid in these calculations, the Abraham model correlations were developed for more than 130 different water-to-organic solvent:

$$\log P \text{ or } \log (C_{S,organic}/C_{S,water}) = c_p + e_p \times \mathbf{E} + s_p \times \mathbf{S} + a_p \times \mathbf{A} + b_p \times \mathbf{B} + v_p \times \mathbf{V} \quad (1)$$

and more than 130 different gas-to-organic solvent solute transfer process:

$$\log K \text{ or } \log (C_{S,organic}/C_{S,gas}) = c_k + e_k \times \mathbf{E} + s_k \times \mathbf{S} + a_k \times \mathbf{A} + b_k \times \mathbf{B} + l_k \times \mathbf{L} \quad (2)$$

Each solute transfer process describes either the logarithm of a water-to-organic solvent partition coefficient, log P, the logarithm of a gas-to-organic solvent partition coefficient, log K, or the logarithm of molar solubility ratios, log ($C_{S,organic}/C_{S,water}$) and log ($C_{S,organic}/C_{S,gas}$), in terms of the product of solute descriptor values (**E**, **S**, **A**, **B**, **V** and **L**) multiplied by the numerical values of complementary solvent/process equation coefficients (c_p, e_p, s_p, a_p, b_p, v_p, c_k, e_k, s_k, a_k, b_k and l_k). Solute descriptors are described as follows: **V** represents the characteristic McGowan molar volume, **L** is the logarithm of the solute's measured gas-to-hexadecane partition coefficient determined at 298 K, **E** is the solute excess molar refractivity relative to that of a linear alkane of comparable molecular volume, **A** and **B** denote the solute's overall hydrogen bond acidity and basicity, respectively, and **S** refers to the solute's dipolarity/polarizability character.

Each product represents a specific type of solute–solvent interaction that is believed to govern the solute transfer process. The sign and magnitude of each product determines whether or not the molecular interaction favors or hinders solute transfer into the organic solvent. For example, in the case of the two hydrogen-bonding terms a positive numerical value of $a_k \times \mathbf{A}$ and/or $b_k \times \mathbf{B}$ corresponds to an increase in the given partition coefficient or increase in the solute's molar concentration in the organic phase, $C_{S,organic}$. Conversely, a negative value of either term results in smaller solute partition coefficients or greater relative solute molar solubility in the aqueous, $C_{S,water}$, and relative molar gas phase concentration, $C_{S,gas}$. Partition coefficients and molar solubility ratios are similarly affected by excess polarizability portion of solute-solvent interactions resulting from the n- and π-electrons, $e \times \mathbf{E}$, the dipolarity/polarizability term, $s \times \mathbf{S}$, and the cavity formation terms, $v_p \times \mathbf{V}$ and $l_k \times \mathbf{L}$, in the two Abraham model expressions.

When interpreting how the various types of molecular interactions affect solute transfer remember that the coefficients represent the difference in the properties of the destination phase minus those in the origination phase. This is the reason why many of the a_p coefficients and all of the b_p coefficients are negative for the water-to-organic solvent transfer processes listed in Table 2. Even for those organic solvents that can engage in H-bond formation water still possess more H-bond donor character than the organic solvent. Hydrogen-bonding solutes prefer to remain in the aqueous phase if not for the positive contributions from the $v_p \times \mathbf{V}$ cavity formation term. These are considerations that one

considers when designing a biphasic aqueous-organic extraction system to remove organic solutes from aqueous solutions.

The equation coefficients for the various Abraham model solute transfer processes used in the current study are tabulated in the last seven columns of Table 2. Each individual transfer process is designated as either "wet", "dry" or "both", depending on whether the organic solvent is in direct contact with the aqueous phase as would be the case for a direct, practical partitioning system. The equation coefficients for the "wet" water-to-organic solvent solute transfer process pertains to the solute partitioning between an aqueous phase saturated with the organic solvent and an organic phase saturated with water. In the case of the "dry" solute transfer processes, the aqueous and the organic phase are not in direct contact with one another, and molar solubility ratios are used to quantify the extent of solute transfer. The "dry" solute transfer correlations can be used to predict the solubility of the solute in additional organic solvents as might be needed in selecting an organic solvent to use in a chemical synthesis or for purifying synthesized compound by recrystallization. For solvents that are almost completely immiscible with water, such as cyclohexane and methylcyclohexane, the designation of "both" is used in Table 2 because the coefficients can be used to describe log $C_{S,organic}/C_{S,water}$, as well as the logarithm of the practical water-to-organic solvent partition coefficient. The presence of small amounts of water in the organic solvent, and small amounts of organic solvent in water, does not affect the solubilizing properties of either water or the organic mono-solvent. Interested readers can find a more detailed discussion of the Abraham model in several informative review articles and book chapters [56–61].

Table 2. Abraham Model Equation Coefficients for Various Water-to-Organic Solvent, Equation (1), and Gas-to-Organic Solvent, Equation (2), Solute Transfer Process [a].

Solvent	*c*	*e*	*s*	*a*	*b*	*l*	*v*
Equation (1) Coefficients							
1-Octanol (wet)	0.088	0.562	−1.054	0.034	−3.460	0.000	3.814
Cyclohexane (both)	0.159	0.784	−1.678	−3.740	−4.929	0.000	4.577
Methylcyclohexane (both)	0.246	0.782	−1.982	−3.517	−4.293	0.000	4.528
Methanol (dry)	0.276	0.334	−0.714	0.243	−3.320	0.000	3.549
Ethanol (dry)	0.222	0.471	−1.035	0.326	−3.596	0.000	3.857
1-Propanol (dry)	0.139	0.405	−1.029	0.247	−3.767	0.000	3.986
1-Butanol (dry)	0.165	0.401	−1.011	0.056	−3.958	0.000	4.044
1-Pentanol (dry)	0.150	0.536	−1.229	0.141	−3.864	0.000	4.077
1-Heptanol (dry)	0.035	0.398	−1.063	0.002	−4.342	0.000	4.317
2-Propanol (dry)	0.099	0.344	−1.049	0.406	−3.827	0.000	4.033
2-Butanol (dry)	0.127	0.253	−0.976	0.158	−3.882	0.000	4.114
2-Methyl-1-propanol (dry)	0.188	0.354	−1.127	0.016	−3.568	0.000	3.986
3-Methyl-1-butanol (dry)	0.073	0.360	−1.273	0.090	−3.770	0.000	4.273
2-Pentanol (dry)	0.115	0.455	−1.331	0.206	−3.745	0.000	4.201
2-Methyl-1-butanol (dry)	0.143	0.388	−1.173	−0.024	−3.817	0.000	4.129
4-Methyl-2-pentanol (dry)	0.096	0.301	−1.100	0.039	−4.081	0.000	4.242
Cyclopentanol (dry)	0.332	0.522	−1.034	−0.106	−3.756	0.000	3.892
Methyl acetate (dry)	0.351	0.223	−0.150	−1.035	−4.527	0.000	3.972
Ethyl acetate (dry)	0.328	0.314	−0.348	−0.847	−4.899	0.000	4.142
Propyl acetate (dry)	0.362	0.280	−0.390	−0.975	−4.928	0.000	4.183
Butyl acetate (dry)	0.289	0.336	−0.501	−0.913	−4.964	0.000	4.262
Pentyl acetate (dry)	0.182	0.261	−0.474	−1.017	−4.952	0.000	4.388
Gas-to-water	−0.994	0.577	2.549	3.813	4.841	0.000	−0.869

Table 2. *Cont.*

Solvent	*c*	*e*	*s*	*a*	*b*	*l*	*v*
Equation (2) Coefficients							
1-Octanol (wet)	−0.198	0.002	0.709	3.519	1.429	0.858	0.000
Cyclohexane (both)	0.163	−0.110	0.000	0.000	0.000	1.013	0.000
Methylcyclohexane (both)	0.318	−0.215	0.000	0.000	0.000	1.012	0.000
Methanol (dry)	−0.039	−0.338	1.317	3.826	1.396	0.773	0.000
Ethanol (dry)	0.017	−0.232	0.867	3.894	1.192	0.846	0.000
1-Propanol (dry)	−0.042	−0.246	0.749	3.888	1.076	0.874	0.000
1-Butanol (dry)	−0.004	−0.285	0.768	3.705	0.879	0.890	0.000
1-Pentanol (dry)	−0.002	−0.161	0.535	3.778	0.960	0.900	0.000
1-Heptanol (dry)	−0.056	−0.216	0.554	3.596	0.803	0.933	0.000
2-Propanol (dry)	−0.048	−0.324	0.713	4.036	1.055	0.884	0.000
2-Butanol (dry)	−0.034	−0.387	0.719	3.736	1.088	0.905	0.000
2-Methyl-1-propanol (dry)	−0.003	−0.357	0.699	3.595	1.247	0.881	0.000
3-Methyl-1-butanol (dry)	−0.052	−0.430	0.628	3.661	0.932	0.937	0.000
2-Pentanol (dry)	−0.031	−0.325	0.496	4.792	1.024	0.934	0.000
2-Methyl-1-butanol (dry)	−0.055	−0.348	0.601	3.565	0.996	0.925	0.000
4-Methyl-2-pentanol (dry)	−0.013	−0.606	0.687	3.622	0.436	0.985	0.000
Cyclopentanol (dry)	−0.151	−0.314	0.693	3.549	0.914	0.956	0.000
Methyl acetate (dry)	0.134	−0.477	1.749	2.678	0.000	0.876	0.000
Ethyl acetate (dry)	0.171	−0.403	1.428	2.726	0.000	0.914	0.000
Propyl acetate (dry)	0.246	−0.346	1.318	2.537	0.000	0.916	0.000
Butyl acetate (dry)	0.154	−0.439	1.223	2.586	0.000	0.953	0.000
Pentyl acetate (dry)	0.154	−0.424	1.172	2.506	0.000	0.962	0.000
Gas-to-water	−1.271	0.822	2.743	3.904	4.814	−0.213	0.000

[a] Equation coefficients for additional organic mono-solvents can be found in cited reference [49]. Coefficients for ionic liquid solvents can be found in a compilation by Jiang and coworkers [62].

All experimental solubility data for vitamin K4, including the measured values given in Table 1 of this study, is reported as mole fraction concentrations. The Abraham model correlations that are available for solute descriptor determinations pertain to molar solubility ratios. The conversion of mole fraction solubilities to molar solubilities is achieved by:

$$C_{S,organic} \approx x_{S,organic}/[x_{S,organic}\ V_{Solute} + (1 - x_{S,organic})\ V_{Solvent}] \quad (3)$$

Dividing the measured $x_{S,organic}$ values by the ideal molar volume of the saturated solution solution. A value of V_{solute} = 0.2205 L mol^{-1} was used for the molar volume of vitamin K4. The solubility of vitamin K4 is sufficiently small in each of the organic mono-solvents considered so that the first term in the denominator, e.g., $x_{S,organic}\ V_{Solute}$, makes an insignificant contribution in the calculation. The molar solubilities and respective solvent equation coefficients are now substituted into Equations (1) and (2). Based on measured solubility data we now have 21 log ($C_{S,organic}/C_{S,water}$) equations and 21 log ($C_{S,organic}/C_{S,gas}$) equations to use in the solute descriptor computations.

There are two additional Abraham model log ($C_{S,water}/C_{S,gas}$) equations to use in our solute descriptor computations that describe the gas-to-water solute transfer process (coefficients given in the last row of the first and second section of entries in Table 2 entries):

$$\log (C_{S,water}/C_{S,gas}) = -0.994 + 0.577\ \mathbf{E} + 2.549\ \mathbf{S} + 3.813\ \mathbf{A} + 4.841\ \mathbf{B} - 0.869\ \mathbf{V} \quad (4)$$

$$\log (C_{S,water}/C_{S,gas}) = -1.271 + 0.822\ \mathbf{E} + 2.743\ \mathbf{S} + 3.904\ \mathbf{A} + 4.814\ \mathbf{B} - 0.213\ \mathbf{L} \quad (5)$$

plus the two equations based on the water-to-wet 1-octanol transfer process. We use an estimated value of log P = 3.590 [63] for the practical water-to-1-octanol partition coefficient of vitamin K4. In total there are 46 mathematical expressions that can be used in the regression analysis for determining vitamin K4′s six solute descriptors (**E**, **S**, **A**, **B**, **V** and **L**) plus the numerical values of log $C_{S,water}$ and log $C_{S,gas}$ needed to calculate the molar

solubility ratios. In our search of the published chemical literature, we did not find an experimental value for the solubility of vitamin K4 in water.

The number of equations is more than sufficient to obtain a set of numerical values having predictive capabilities. Fortunately, three of the six solute descriptors can be calculated solely from molecular structure considerations. The **E** solute descriptor was taken as **E** = 1.500 [45], the **A** solute descriptor was set equal to zero because vitamin K4 does not possess a hydrogen atom that is capable of acting as an H-bond donor, and the McGowan molecular volume descriptor, **V** = 1.9387, was calculated from the number of chemical bonds, as well as the same number and atomic volumes of carbon, hydrogen, oxygen, nitrogen and fluorine atoms [64]. The 46 Abraham model expressions were then solved simultaneously using the built-in Solver add-in feature on Microsoft Excel to give: numerical values of the remaining three solute descriptors: **S** = 2.143; **B** = 0.760; and **L** = 9.931, plus the molar concentrations of log $C_{S,water}$ = −4.560 and log $C_{S,gas}$ = −11.891, needed for the molar solubility calculations. The overall standard deviation associated with the regression analysis was SD = 0.110 log units. Individual standard deviations were SD = 0.118 log units and SD = 0.105 log units for the 23 calculated and observed log ($C_{S,organic}/C_{S,water}$) values and the 23 calculated and observed log ($C_{S,organic}/C_{S,gas}$) values, respectively. Deviations between the observed and back-calculated values of log *P* and log *K* for solute transfer into wet 1-octanol are included in the respective standard errors for the log ($C_{S,organic}/C_{S,water}$) and log ($C_{S,organic}/C_{S,gas}$) results. Compared to vitamin K3 (menadione) whose experiment-based solute descriptors of: **E** = 1.250; **S** = 1.480; **A** = 0.000; **B** = 0.540; **V** = 1.2007; and **L** = 6.766, which were previously determined by Liu et al. [65] using the published solubility data in several organic mono-solvents and binary aqueous-alcohol mixtures [66–68], vitamin K4 exhibits much greater polarity/polarizability and slightly more H-bond basicity than its parent menadione. The increased H-bond basicity likely results from the two lone electron pairs on each of the two additional oxygen atoms (see Figure 1 for the molecular structure of both vitamins).

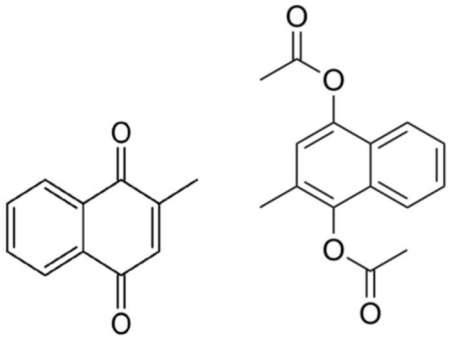

Figure 1. Molecular structures of vitamin K3 and vitamin K4.

There is very little published information regarding the physical, chemical, thermodynamic and pharmacokinetic properties of vitamin K4. The experiment-based solute descriptors that were just determined for vitamin K4 can now be used in conjunction with previously published Abraham model correlations to predict the vitamin's molar solubility in more than 100 different dry organic mono-solvents [23–27,49] and in more than 90 different ionic liquids [62], and to predict practical partition coefficients for many different biphasic aqueous-organic solvent extraction systems [49,69–72]. The Abraham model correlations have also been developed for predicting the vapor pressure [73], standard molar enthalpies of vaporization [74] and sublimation [75] of organic compounds at 298.15 K, enthalpies of solvation of organic compounds dissolved in both water [76] and in more than 30 organic solvents of varying polarity and hydrogen-bonding character [77–80], as well as a compound's blood-to-body fluid/tissue and air-to-body fluid/partition coefficients at 310 K [30–32,36–38,81,82]. The predicted values are obtained by simply substituting the

numerical values of the compound's solute descriptors into previously published Abraham model correlations. For example, we calculate numerical values of −116 kJ mol^{-1} and −80 kJ mol^{-1} for the standard molar enthalpies of solvation of vitamin K4 dissolved in 1,4-dioxane and water at 298 K [77], respectively, and the estimated equilibrium vapor pressure, VP, above the solid vitamin is VP = 6.2 × 10^{-12} atm at 298 K [73]. In Table 3 we list the coefficients for several in vivo blood-to-rat tissue partitioning process at 310 K [81], along with the respective predicted log *P* value for vitamin K4. Calculations indicate that vitamin K4 is distributed primarily to the fat tissues of the rat, followed by the skin, lung, kidney and brain. All calculated blood-to-tissue partition coefficients exceed unity, with the blood-to-liver value being the smallest value at *P* = 1.05.

Table 3. Equations for predicting the logarithm of in vivo blood-to-rat tissue partition coefficients and the calculated log *P* values for vitamin K4.

System	c_p	e_p	s_p	a_p	b_p	v_p	Calculated
Blood-to-brain	0.547	0.221	−0.604	−0.641	−0.681	0.635	0.298
Blood-to-muscle	0.082	−0.059	0.010	−0.248	0.028	0.110	0.249
Blood-to-liver	0.292	0.000	−0.296	−0.334	0.181	0.337	0.022
Blood-to-lung	0.269	0.000	−0.523	−0.723	0.000	0.720	0.544
Blood-to-kidney	0.494	−0.067	−0.426	−0.367	0.232	0.410	0.452
Blood-to-heart	0.132	−0.039	−0.394	−0.376	0.009	0.527	0.258
Blood-to-skin	−0.105	−0.117	0.034	0.000	−0.681	0.756	0.756
Blood-to-fat	0.077	0.249	−0.215	−0.902	−1.523	1.234	1.225

4. Summary

The Abraham general solvation parameter model has been shown to provide a reasonably accurate mathematical description of the observed solubility behavior of vitamin K4 dissolved in 2 cyclic hydrocarbon solvents (cyclohexane, methylcyclohexane), 14 alcohol solvents (methanol, ethanol, 1-propanol, 1-butanol, 1-pentanol, 1-heptanol, 2-propanol, 2-butanol, 2-methyl-1-propanol, 3-methyl-1-butanol, 2-pentanol, 2-methyl-1-butanol, 4-methyl-2-pentanol, cyclopentanol), and five alkyl acetate solvents (methyl acetate, ethyl acetate, propyl acetate, butyl acetate, pentyl acetate) at 298.15 K. The back-calculated molar solubility ratios based on our derived solute descriptors differ from the experimental values by an approximate overall standard deviation of 0.110 log units. The small difference between the observed and back-calculated values suggests that the calculated descriptor values reported in the present communication will enable one to successfully estimate the solubility of vitamin K4 in the additional 130 or so organic mono-solvents and binary aqueous-organic solvent mixtures for which the Abraham model correlations have been determined. The calculated solute descriptors further indicate that vitamin K4 exhibits much greater polarity/polarizability and slightly more H-bond basicity than its parent menadione. The increased H-bond basicity likely results from the two lone electron pairs on each of the two additional oxygen atoms.

The solute descriptors reported in the current study can be used to predict the vapor pressure of vitamin K4 at 298 K, as well as the compound's standard molar enthalpies of vaporization and sublimation. Important pharmaceutical properties that can be predicted include the logarithm of the in vivo blood-to-rat tissue partition coefficients. Calculations indicate that vitamin K4 is distributed primarily to the fat tissues of the rat, followed by the skin, lung, kidney, and brain. All predicted blood-to-tissue partition coefficients exceed unity, with the blood-to-liver value being the smallest value at *P* = 1.05.

Author Contributions: Conceptualization, writing—original draft preparation, W.E.A.J.; data acquisition; S.M., R.M. and T.K.; formal data analysis, S.M., R.M. and T.K.; writing—review and editing, S.M., R.M. and T.K. All authors have read and agreed to the published version of the manuscript.

Funding: The research received no external funding.

Data Availability Statement: Data are contained within the manuscript.

Acknowledgments: Saikiran Motati, Ramya Motati and Trisha Kandi, thank the University of North Texas's Texas Academy of Mathematics and Science (TAMS) program for providing a summer research scholarship award.

Conflicts of Interest: The authors declare no conflict of interest.

References

1. Avdeef, A.; Kansy, M. Trends in PhysChem properties of newly approved drugs over the last six years; Predicting solubility of drugs approved in 2021. *J Solut. Chem.* **2022**, *51*, 1455–1481. [CrossRef]
2. Avdeef, A.; Kansy, M. Predicting solubility of newly-approved drugs (2016–2020) with a simple ABSOLV and GSE(flexible-acceptor) consensus model outperforming random forest regression. *J. Solut. Chem.* **2022**, *51*, 1020–1055. [CrossRef] [PubMed]
3. Avdeef, A. Cocrystal solubility product prediction using an *in combo* model and simulations to improve design of experiments. *Pharm. Res.* **2018**, *35*, 40. [CrossRef] [PubMed]
4. Shu, C.-C.; Lin, S.-T. Prediction of drug solubility in mixed solvent systems using the COSMO-SAC activity coefficient model. *Ind. Eng. Chem. Res.* **2011**, *50*, 142–147. [CrossRef]
5. Klamt, A.; Eckert, F.; Hornig, M.; Beck, M.E.; Burger, T. Prediction of aqueous solubility of drugs and pesticides with COSMO-RS. *J. Comput. Chem.* **2002**, *23*, 275–281. [CrossRef]
6. Silva, F.; Veiga, F.; Rodrigues, S.P.J.; Cardoso, C.; Paiva-Santos, A.C. COSMO models for the pharmaceutical development of parenteral drug formulations. *Eur. J. Pharm. Biopharm.* **2023**, *187*, 156–165. [CrossRef]
7. Mahmoudabadi, S.Z.; Pazuki, G. A predictive PC-SAFT EOS based on COSMO for pharmaceutical compounds. *Sci. Rep.* **2021**, *11*, 6405. [CrossRef]
8. Lusci, A.; Pollastri, G.; Baldi, P. Deep architectures and deep learning in chemoinformatics: The prediction of aqueous solubility for drug-like molecules. *J. Chem. Inf. Model.* **2013**, *53*, 1563–1575. [CrossRef]
9. Boobier, S.; Hose, D.R.J.; Blacker, A.J.; Nguyen, B.N. Machine learning with physicochemical relationships: Solubility prediction in organic solvents and water. *Nat. Commun.* **2020**, *11*, 5753. [CrossRef]
10. Cysewski, P.; Jeliński, T.; Przybyłek, M. Application of COSMO-RS-DARE as a tool for testing consistency of solubility data: Case of coumarin in neat alcohols. *Molecules* **2022**, *27*, 5274. [CrossRef]
11. Rahimpour, E.; Xu, R.; Zhao, H.; Acree, W.E., Jr.; Jouyban, A. Simulation of clozapine solubility in mono- and mixed solvents at different temperatures. *J. Solut. Chem.* **2022**, *51*, 1540–1570. [CrossRef]
12. Jouyban, A. Review of the cosolvency models for predictiong drug solubility in solvent mixtures: An update. *J. Pharm. Pharm. Sci.* **2019**, *22*, 466–485. [CrossRef]
13. Bergström, C.A.S.; Larsson, P. Computational prediction of drug solubility in water-based systems: Qualitative and quantitative approaches used in the current drug discovery and development setting. *Int. J. Pharm.* **2018**, *540*, 185–193. [CrossRef] [PubMed]
14. Benavides, D.; Longacre, L.; Varadharajan, A.; Acree, W.E., Jr. Calculation of Abraham model solute descriptors for 2-naphthoxyacetic acid. *Phys. Chem. Liq.* **2023**, *61*, 264–274. [CrossRef]
15. Yao, E.; Zhou, A.; Wu, S.; Shanmugam, N.; Varadharajan, A.; Sinha, S.; Wu, E.; Acree, W.E., Jr. Determination of Abraham model solute descriptors for *N*-hydroxyphthalimide: An organic compound having a *N*-hydroxy (N-OH) functional group. *J. Solut. Chem.* **2023**, *52*, 895–909. [CrossRef]
16. Sinha, S.; Varadharajan, A.; Xu, A.; Wu, E.; Acree, W.E., Jr. Determination of Abraham model solute descriptors for hippuric acid from measured molar solubilities in several organic mono-solvents of varying polarity and hydrogen-bonding ability. *Phys. Chem. Liq.* **2022**, *60*, 563–571. [CrossRef]
17. Lee, G.; Che, M.; Qian, E.; Wang, L.; Gupta, A.; Neal, R.; Yue, D.; Downs, S.; Mayes, T.; Rose, O.; et al. Determination of Abraham model solute descriptors for o-acetoacetanisidide based on experimental solubility data in organic mono-solvents. *Phys. Chem. Liq.* **2019**, *57*, 528–535. [CrossRef]
18. Yao, X.; Wang, Z.; Geng, Y.; Zhao, H.; Rahimpour, E.; Acree, W.E., Jr.; Jouyban, A. Hirshfeld surface and electrostatic potential surface analysis of clozapine and its solubility and molecular interactions in aqueous blends. *J. Mol. Liq.* **2022**, *360*, 119328. [CrossRef]
19. Liu, Y.; Zhao, H.; Farajtabar, A.; Zhu, P.; Rahimpour, E.; Acree, W.E., Jr.; Jouyban, A. Acetamiprid in several binary aqueous solutions: Solubility, intermolecular interactions and solvation behavior. *J. Chem. Thermodyn.* **2022**, *172*, 106828. [CrossRef]
20. Liu, F.; Zhao, H.; Farajtabar, A.; Zhu, P.; Jouyban, A.; Acree, W.E., Jr. Quantitative surface analysis of paclobutrazol molecule and comprehensive insight into its solubility in aqueous co-solvent solutions. *J. Chem. Thermodyn.* **2022**, *170*, 106787. [CrossRef]
21. Akay, S.; Kayan, B.; Coskun, S.; Jouyban, A.; Martinez, F.; Acree, W.E., Jr. Equilibrium solubility of 6-methylcoumarin in some (ethanol + water) mixtures: Determination, correlation, thermodynamics and preferential solvation. *Phys. Chem. Liq.* **2022**, *60*, 707–727. [CrossRef]
22. Cardenas-Torres, R.E.; Ortiz, C.P.; Acree, W.E., Jr.; Jouyban, A.; Martinez, F.; Delgado, D.R. Thermodynamic study and preferential solvation of sulfamerazine in acetonitrile + methanol cosolvent mixtures at different temperatures. *J. Mol. Liq.* **2022**, *349*, 118172. [CrossRef]

23. Varadharajan, A.; Sinha, S.; Xu, A.; Daniel, A.; Kim, K.; Shanmugam, N.; Wu, E.; Yang, C.; Zhang, M.; Acree, W.E., Jr. Development of Abraham model correlations for describing solute transfer into transcutol based on molar solubility ratios for pharmaceutical and other organic compounds. *J. Solut. Chem.* **2023**, *52*, 70–90. [CrossRef]
24. Xu, A.; Varadharajan, A.; Shanmugam, N.; Kim, K.; Huang, E.; Cai, S.K.; Acree, W.E., Jr. Abraham model description of the solubilising properties of the isopropyl acetate organic mono-solvent. *Phys. Chem. Liq.* **2022**, *60*, 312–324. [CrossRef]
25. Cai, S.K.; Huang, E.; Kim, K.; Shanmugam, N.; Varadharajan, A.; Xu, A.; Acree, W.E., Jr. Development of Abraham model correlations for solute transfer into cyclopentanol from both water and the gas phase based on measured solubility ratios. *Phys. Chem. Liq.* **2022**, *60*, 287–296. [CrossRef]
26. Strickland, S.; Ocon, L.; Zhang, A.; Wang, S.; Eddula, S.; Liu, G.; Tirumala, P.; Huang, J.; Dai, J.; Jiang, C.; et al. Abraham model correlations for describing dissolution of organic solutes and inorganic gases in dimethyl carbonate. *Phys. Chem. Liq.* **2021**, *59*, 181–195. [CrossRef]
27. Sedov, I.A.; Salikov, T.M.; Qian, E.; Wadawadigi, A.; Zha, O.; Acree, W.E., Jr.; Abraham, M.H. Abraham model correlations for solute transfer into 2-methyl-2-butanol based on measured activity coefficient and solubility data at 298.15 K. *J. Mol. Liq.* **2019**, *293*, 111454. [CrossRef]
28. Zhang, K.; Chen, M.; Scriba, G.K.E.; Abraham, M.H.; Fahr, A.; Liu, X. Human skin permeation of neutral species and ionic species: Extended linear free-energy relationship analyses. *J. Pharm. Sci.* **2012**, *101*, 2034–2044. [CrossRef]
29. Abraham, M.H.; Martins, F. Human skin permeation and partition: General linear free-energy relationship analyses. *J. Pharm. Sci.* **2004**, *93*, 1508–1523. [CrossRef]
30. Sprunger, L.M.; Gibbs, J.; Acree, W.E., Jr.; Abraham, M.H. Correlation of human and animal air-to-blood partition coefficients with a single linear free energy relationship model. *QSAR Comb. Sci.* **2008**, *27*, 1130–1139. [CrossRef]
31. Abraham, M.H.; Ibrahim, A.; Acree, W.E., Jr. Air to lung partition coefficients for volatile organic compounds and blood to lung partition coefficients for volatile organic compounds and drugs. *Eur. J. Med. Chem.* **2008**, *43*, 478–485. [CrossRef] [PubMed]
32. Abraham, M.H.; Ibrahim, A.; Acree, W.E., Jr. Air to muscle and blood/plasma to muscle distribution of volatile organic compounds and drugs: Linear free energy analyses. *Chem. Res. Toxicol.* **2006**, *19*, 801–808. [CrossRef] [PubMed]
33. Abraham, M.H.; Hassanisadi, M.; Jalali-Heravi, M.; Ghafourian, T.; Cain, W.S.; Cometto-Muniz, J.E. Draize rabbit eye test compatibility with eye irritation thresholds in humans: A quantitative structure-activity relationship analysis. *Toxicol. Sci.* **2003**, *76*, 384–391. [CrossRef] [PubMed]
34. Abraham, M.H. Human intestinal absorption-neutral molecules and ionic species. *J. Pharm. Sci.* **2014**, *103*, 1956–1966. [CrossRef]
35. Zhao, Y.H.; Le, J.; Abraham, M.H.; Hersey, A.; Eddershaw, P.J.; Luscombe, C.N.; Boutina, D.; Beck, G.; Sherborne, B.; Cooper, I.; et al. Evaluation of human intestinal absorption data and subsequent derivation of a quantitative structure-activity relationship (QSAR) with the Abraham descriptors. *J. Pharm. Sci.* **2001**, *90*, 749–784. [CrossRef] [PubMed]
36. Abraham, M.H.; Ibrahim, A. Air to fat and blood to fat distribution of volatile organic compounds and drugs: Linear free energy analyses. *Eur. J. Med. Chem.* **2006**, *41*, 1430–1438. [CrossRef]
37. Abraham, M.H.; Ibrahim, A.; Zhao, Y.; Acree, W.E., Jr. A data base for partition of volatile organic compounds and drugs from blood/plasma/serum to brain, and an LFER analysis of the data. *J. Pharm. Sci.* **2006**, *95*, 2091–2100. [CrossRef]
38. Abraham, M.H.; Ibrahim, A.; Acree, W.E., Jr. Air to brain, blood to brain and plasma to brain distribution of volatile organic compounds: Linear free energy analyses. *Eur. J. Med. Chem.* **2006**, *41*, 494–502. [CrossRef]
39. He, J.; Abraham, M.H.; Acree, W.E., Jr.; Zhao, Y.H. A linear free energy analysis of PAMPA models for biological systems. *Int. J. Pharm.* **2015**, *496*, 717–722. [CrossRef]
40. Soriano-Meseguer, S.; Fuguet, E.; Port, A.; Rosés, M. Evaluation of the ability of PAMPA membranes to emulate biological processes through the Abraham solvation parameter model. *Membranes* **2023**, *13*, 640. [CrossRef]
41. Henneberger, L.; Goss, K.-U.; Endo, S. Partitioning of organic ions to muscle protein: Experimental data, modeling, and implications for in Vivo distribution of organic ions. *Environ. Sci. Technol.* **2016**, *50*, 7029–7036. [CrossRef] [PubMed]
42. Endo, S.; Goss, K.-U. Serum albumin binding of structurally diverse neutral organic compounds: Data and models. *Chem. Res. Toxicol.* **2011**, *24*, 2293–2301. [CrossRef] [PubMed]
43. Li, J. Evaluation of blood simulating solvents in extractables and leachables testing for chemical characterization of medical devices based on Abraham general solvation model. *J. Mol. Liq.* **2022**, *345*, 116995. [CrossRef]
44. Li, J. Evaluation of fatty tissue representative solvents in extraction of medical devices for chromatographic analysis of devices' extractables and leachables based on Abraham general solvation model. *J. Chromatogr. A* **2022**, *1676*, 463240. [CrossRef]
45. Ulrich, N.; Endo, S.; Brown, T.N.; Watanabe, N.; Bronner, G.; Abraham, M.H.; Goss, K.-U. UFZ-LSER Database v 3.2.1 Internet. Leipzig, Germany, Helmholtz Centre for Environmental Research-UFZ. 2017. Available online: http://www.ufz.de/lserd (accessed on 27 May 2023).
46. Chung, Y.; Vermeire, F.H.; Wu, H.; Walker, P.J.; Abraham, M.H.; Green, W.H. Group contribution and machine learning approaches to predict Abraham solute parameters, solvation free energy, and solvation enthalpy. *J. Chem. Inf. Model.* **2022**, *62*, 433–446. [CrossRef]
47. Solvation Tools. Available online: https://rmg.mit.edu/database/solvation/search/ (accessed on 1 August 2023).
48. Acree, W.E., Jr.; Smart, K.; Abraham, M.H. Abraham model solute descriptors reveal strong intramolecular hydrogen bonding in 1,4-dihydroxyanthraquinone and 1,8-dihydroxyanthraquinone. *Phys. Chem. Liq.* **2018**, *56*, 416–420. [CrossRef]

49. Sinha, S.; Yang, C.; Wu, E.; Acree, W.E., Jr. Abraham solvation parameter model: Examination of possible intramolecular hydrogen-bonding using calculated solute descriptors. *Liquids* **2022**, *2*, 131–146. [CrossRef]
50. Yao, E.; Acree, W.E., Jr. Abraham model solute descriptors for favipiravir: Case of tautomeric equilibrium and intramolecular hydrogen-bond formation. *Thermo* **2023**, *3*, 443–451. [CrossRef]
51. Jiang, Y.; Yang, J.; Yang, C.; Meng, F.; Zhou, Y.; Yu, B.; Khan, M.; Yang, H. Vitamin K4 induces tumor cytotoxicity in human prostate carcinoma PC-3 cells via the mitochondria-related apoptotic pathway. *Pharmazie* **2013**, *68*, 442–448. [CrossRef]
52. Di, W.; Khan, M.; Gao, Y.; Cui, J.; Wang, D.; Qu, M.; Feng, L.; Maryam, A.; Gao, H. Vitamin K4 inhibits the proliferation and induces apoptosis of U2OS osteosarcoma cells via mitochondrial dysfunction. *Mol. Med. Rep.* **2017**, *15*, 277–284. [CrossRef]
53. Lu, X.; Yang, X.; Wu, X.; Wang, J.; Zhao, Z. Determination and simulation of menadiol diacetate solubility in 14 solvents at temperatures from 283.15 to 323.15 K. *J. Chem. Eng. Data* **2023**, *68*, 977–993. [CrossRef]
54. Charlton, A.K.; Daniels, C.R.; Acree, W.E., Jr.; Abraham, M.H. Solubility of crystalline nonelectrolyte solutes in organic solvents: Mathematical correlation of acetylsalicylic acid solubilities with the Abraham general solvation model. *J. Solut. Chem.* **2003**, *32*, 1087–1102. [CrossRef]
55. De Fina, K.M.; Ezell, C.; Acree, W.E., Jr. Solubility of ferrocene in organic nonelectrolyte solvents. Comparison of observed versus predicted values based upon mobile order theory. *Phys. Chem. Liq.* **2001**, *39*, 699–710. [CrossRef]
56. Jalan, A.; Ashcraft, R.W.; West, R.H.; Green, W.H. Predicting solvation energies for kinetic modeling. *Annu. Rep. Prog. Chem. Sec. C Phys. Chem.* **2010**, *106*, 211–258. [CrossRef]
57. Clarke, E.D.; Mallon, L. The determination of Abraham descriptors and their application to crop protection research. In *Modern Methods in Crop Protection Research*; Jeschke., P., Krämer, W., Schirmer, U., Witschel, M., Eds.; Wiley: New York, NY, USA, 2012.
58. Clarke, E.D. Beyond physical properties–application of Abraham descriptors and LFER analysis in agrochemical research. *Bioorg. Med. Chem.* **2010**, *17*, 4153–4159. [CrossRef]
59. Poole, C.F.; Ariyasena, T.C.; Lenca, N. Estimation of the environmental properties of compounds from chromatographic properties and the solvation parameter method. *J. Chromatogr. A* **2013**, *1317*, 85–104. [CrossRef]
60. Poole, C.F.; Atapattu, S.N. Recent advances for estimating environmental properties for small molecules from chromatographic measurements and the solvation parameter model. *J. Chromatogr. A* **2023**, *1687*, 463682. [CrossRef]
61. Endo, S.; Goss, K.-U. Applications of polyparameter linear free energy relationships in environmental chemistry. *Environ. Sci. Technol.* **2014**, *48*, 12477–12491. [CrossRef]
62. Jiang, B.; Horton, M.Y.; Acree, W.E., Jr.; Abraham, M.H. Ion-specific equation coefficient version of the abraham model for ionic liquid solvents: Determination of coefficients for tributylethylphosphonium, 1-butyl-1-methylmorpholinium, 1-allyl-1-methylimidazolium and octyltriethylammonium cations. *Phys. Chem. Liq.* **2017**, *55*, 358–385. [CrossRef]
63. SciFinder. Chemical Abstracts Service. *Columbus, OH, USA.* Available online: https://scifinder.cas.org (accessed on 28 July 2023).
64. Abraham, M.H.; McGowan, J.C. The use of characteristic volumes to measure cavity terms in reversed phase liquid chromatography. *Chromatographia* **1987**, *23*, 243–246. [CrossRef]
65. Liu, X.; Abraham, M.H.; Acree, W.E., Jr. Descriptors for vitamin K3 (menadione); calculation of biological and physicochemical properties. *J. Mol. Liq.* **2021**, *330*, 115707. [CrossRef]
66. Yu, Y.; Li, F.; Long, S.; Xu, L.; Liu, F. Solubility, thermodynamic properties, HSP, and molecular interactions of vitamin K3 in pure solvents. *J. Mol. Liq.* **2020**, *317*, 113945. [CrossRef]
67. Song, C.Y.; Shen, H.Z.; Wang, L.C.; Zhao, J.H.; Wang, F.A. Solubilities of Vitamin K3 in benzene, toluene, ethylbenzene, o-xylene, m-xylene and p-xylene between (299.44 and 344.24) K. *J. Chem. Eng. Data* **2008**, *53*, 283–285. [CrossRef]
68. Song, C.Y.; Shen, H.Z.; Zhao, J.H.; Wang, L.C.; Wang, F.A. Solubilities of 2-methyl-1,4-naphthoquinone in water + (methanol, ethanol, 1-propanol, 2-propanol, 1,2-propanediol and glycerine, respectively) from (293.15 to 337.92) K. *J. Chem. Eng. Data* **2007**, *52*, 2018–2019. [CrossRef]
69. Churchill, B.; Acree, W.E.; Abraham, M.H. Abraham model correlations for direct water-to-2,2,5,5-tetramethyloxolane solute transfer partitioning process revisited. *Phys. Chem. Liq.* **2020**, *58*, 833–838. [CrossRef]
70. Abraham, M.H.; Acree, W.E. Descriptors for the prediction of partition coefficients of 8-hydroxyquinoline and its derivatives. *Sep. Sci. Technol.* **2014**, *49*, 2135–2141. [CrossRef]
71. Smart, K.; Garcia, E.; Oloyede, B.; Fischer, R.; Golden, T.D.; Acree, W.E., Jr.; Abraham, M.H. The partition of organic compounds from water into the methyl isobutyl ketone extraction solvent with updated Abraham model equation. *Phys. Chem. Liq.* **2021**, *59*, 431–441. [CrossRef]
72. Smart, K.; Connolly, E.; Ocon, L.; Golden, T.; Acree, W.E.; Abraham, M.H. Abraham model correlations for describing the partition of organic compounds from water into the methyl ethyl ketone extraction solvent. *Phys. Chem. Liq.* **2022**, *60*, 47–58. [CrossRef]
73. Abraham, M.H.; Acree, W.E., Jr. Estimation of vapor pressures of liquid and solid organic and organometallic compounds at 298.15 K. *Fluid Phase Equilib.* **2020**, *519*, 112595. [CrossRef]
74. Churchill, B.; Acree, W.E., Jr.; Abraham, M.H. Development of Abraham model expressions for predicting the standard molar enthalpies of vaporization of organic compounds at 298.15 K. *Thermochim. Acta* **2019**, *681*, 178372. [CrossRef]
75. Abraham, M.H.; Acree, W.E., Jr. Estimation of heat capacities of gases, liquids and solids, and heat capacities of vaporization and of sublimation of organic chemicals at 298.15 K. *J. Mol. Liq.* **2020**, *317*, 113969. [CrossRef]
76. Mintz, C.; Clark, M.; Acree, W.E., Jr.; Abraham, M.H. Enthalpy of solvation correlations for gaseous solutes dissolved in water and in 1-octanol based on the Abraham model. *J. Chem. Inf. Model.* **2007**, *47*, 115–121. [CrossRef]

77. Hart, E.; Grover, D.; Zettl, H.; Koshevarova, V.; Acree, W.E., Jr.; Abraham, M.H. Development of Abraham model expressions for predicting the enthalpies of solvation of solutes dissolved in acetic acid. *Phys. Chem. Liq.* **2016**, *54*, 141–154. [CrossRef]
78. Magsumov, T.I.; Sedov, I.A.; Acree, W.E., Jr. Development of Abraham model correlations for enthalpies of solvation of solutes dissolved in *N*-methylformamide, 2-pyrrolidone and *N*-methylpyrrolidone. *J. Mol. Liq.* **2021**, *323*, 114609. [CrossRef]
79. Varfolomeev, M.A.; Stolov, M.A.; Nagrimanov, R.N.; Rakipov, I.T.; Acree, W.E., Jr.; Abraham, M.H. Analysis of solute-pyridine intermolecular interactions based on experimental enthalpies of solution and enthalpies of solvation of solutes dissolved in pyridine. *Thermochim. Acta* **2018**, *660*, 11–17. [CrossRef]
80. Stolov, M.A.; Zaitseva, K.V.; Varfolomeev, M.A.; Acree, W.E. Enthalpies of solution and enthalpies of solvation of organic solutes in ethylene glycol at 298 K: Prediction and analysis of intermolecular interaction contributions. *Thermochim. Acta* **2017**, *648*, 91–99. [CrossRef]
81. Abraham, M.H.; Gola, J.M.R.; Ibrahim, A.; Acree, W.E., Jr.; Liu, X. The prediction of blood–tissue partitions, water–skin partitions and skin permeation for agrochemicals. *Pest Manag. Sci.* **2014**, *70*, 1130–1137. [CrossRef]
82. Abraham, M.H.; Gola, J.M.R.; Ibrahim, A.; Acree, W.E., Jr.; Liu, X. A simple method for estimating in vitro air–tissue and in vivo blood–tissue partition coefficients. *Chemosphere* **2015**, *120*, 188–191. [CrossRef]